

# DEPTH-SELECTIVE DIAGNOSTICS OF THERMAL BARRIER COATINGS INCORPORATING THERMOGRAPHIC PHOSPHORS

Jeffrey I. Eldridge and Timothy J. Bencic  
NASA Glenn Research Center  
Cleveland, OH 44135

Stephen W. Allison and David L. Beshears  
Oak Ridge National Laboratory  
Oak Ridge, TN 37831

## KEYWORDS

Thermal Barrier Coatings, Thermographic Phosphors, Temperature Measurement

## ABSTRACT

Thermographic phosphors have been previously demonstrated to provide effective non-contact, emissivity-independent surface temperature measurements. Because of the translucent nature of thermal barrier coatings (TBCs), thermographic-phosphor-based temperature measurements can be extended beyond the surface to provide depth-selective temperature measurements by incorporating the thermographic phosphor layer at the depth where the temperature measurement is desired. In this paper, thermographic phosphor ( $\text{Y}_2\text{O}_3\text{:Eu}$ ) fluorescence decay time measurements are demonstrated for the first time to provide through-the-coating-thickness temperature readings up to  $1000^\circ\text{C}$  with the phosphor layer residing beneath a  $100\text{-}\mu\text{m}$ -thick TBC (plasma-sprayed 8wt% yttria-stabilized zirconia). With an appropriately chosen excitation wavelength and detection configuration, it is shown that sufficient phosphor emission is generated to provide effective temperature measurements, despite the attenuation of both the excitation and emission intensities by the overlying TBC. This depth-selective temperature measurement capability should prove particularly useful for TBC diagnostics, where a large thermal gradient is typically present across the TBC thickness.

## INTRODUCTION

Thermal barrier coatings (TBCs) provide highly beneficial thermal protection for turbine engine components (ref. 1). TBCs are ceramic oxide coatings with low thermal conductivity; the most widely used TBC for turbine engine applications is composed of 8wt% yttria-stabilized zirconia (8YSZ). The measurement of temperature gradients through the TBC is critical to the evaluation of TBC performance and health monitoring as well as to the accurate simulation of thermal gradients in engine environments. Non-contact surface temperature measurements of translucent TBCs in a flame environment have

This report is a preprint of an article submitted to a journal for publication. Because of changes that may be made before formal publication, this preprint is made available with the understanding that it will not be cited or reproduced without the permission of the author.

proven difficult (ref. 2). For example, the application of IR pyrometry to TBCs in an engine environment is problematic because of (1) the interference of reflected radiation and (2) because the TBC translucency at conventional pyrometer wavelengths allows radiation from well below the TBC surface to reach the pyrometer so that surface temperature measurements cannot be obtained. Two approaches have been pursued to surmount these difficulties. One successful approach has been to develop long-wavelength ( $> 10 \mu\text{m}$ ) pyrometers that operate at wavelengths where the TBCs are opaque (to allow surface measurements) and have near-zero reflectance (to minimize interference of reflected radiation), but with the drawback of much lower signal and sensitivity than at shorter wavelengths (refs. 3,4). Another successful approach has been to apply thermographic phosphors to the TBC surface to obtain emissivity-independent surface temperature measurements either by the temperature dependence of the fluorescence decay time or of the ratio of intensities of selected emission lines (refs. 5,6).

One aspect of the potential for using thermographic phosphors for TBC temperature measurements that has not yet been explored is to take advantage of the TBC translucency to place the phosphor not only at the surface, but at any depth where the temperature measurement is desired. The primary obstacle to depth-penetrating measurements is the attenuation of the excitation and emission intensities by the overlying TBC. In particular, YSZ-based TBCs are completely opaque to the UV excitation wavelengths that are normally used for surface temperature measurements. In this paper, it is demonstrated that with an appropriately chosen excitation wavelength and detection configuration, sufficient phosphor emission is generated to achieve through-the-thickness temperature readings up to  $1000^\circ\text{C}$  with the phosphor located beneath a  $100\text{-}\mu\text{m}$ -thick TBC. With further development, the strategic placement of luminescent species through the TBC could add embedded sensing functions to the TBC so that the photon-excited emission would provide information about temperature gradients and coating integrity.

## STRATEGY FOR DEPTH-SELECTIVE TEMPERATURE MEASUREMENTS

The strategy for achieving depth-probing temperature measurements using thermographic phosphors is to select a phosphor that exhibits significant excitation and emission peaks that can be transmitted through the TBC. The most severe aspect of this limitation is to find a phosphor with an excitation peak at sufficiently long wavelengths, since most phosphors are most efficiently excited at UV wavelengths that will not penetrate into the TBC. Figure 1 illustrates the wavelength restriction presented by the overlying TBC by showing the spectral hemispherical transmittance curves for two freestanding plasma-sprayed 8YSZ (PS-8YSZ) coatings with thicknesses of 115 and 195  $\mu\text{m}$ . These curves show that there is no transmittance at UV wavelengths (below 380 nm) and that an excitation wavelength above 500 nm is needed to achieve transmittances of more than a few percent. As shown in Figure 1, the  $\text{Y}_2\text{O}_3\text{:Eu}$  phosphor has been found to meet this requirement with a minor excitation peak at 532 nm as well as an emission peak at 611 nm. While  $\text{Y}_2\text{O}_3\text{:Eu}$  has a much larger wide excitation peak at 267 nm and is most effectively excited by a 266 nm fourth harmonic YAG:Nd laser (refs. 6,7), the 532 nm excitation provides a small, but rare significant excitation at a wavelength where the TBC is reasonably transparent. Fortunately, the 532 nm excitation can be supplied by a second harmonic YAG:Nd laser. While the  $\text{Y}_2\text{O}_3\text{:Eu}$  phosphor was used for all the experiments reported in this paper, it should be noted that additional measurements have shown that YSZ:Eu also exhibits a minor excitation peak at 532 nm. As reported by Feist and Heyes (ref. 6), YSZ:Eu also functions as an effective thermographic phosphor and provides the additional advantage of being introduced into the coating by a more benign low-level

ank

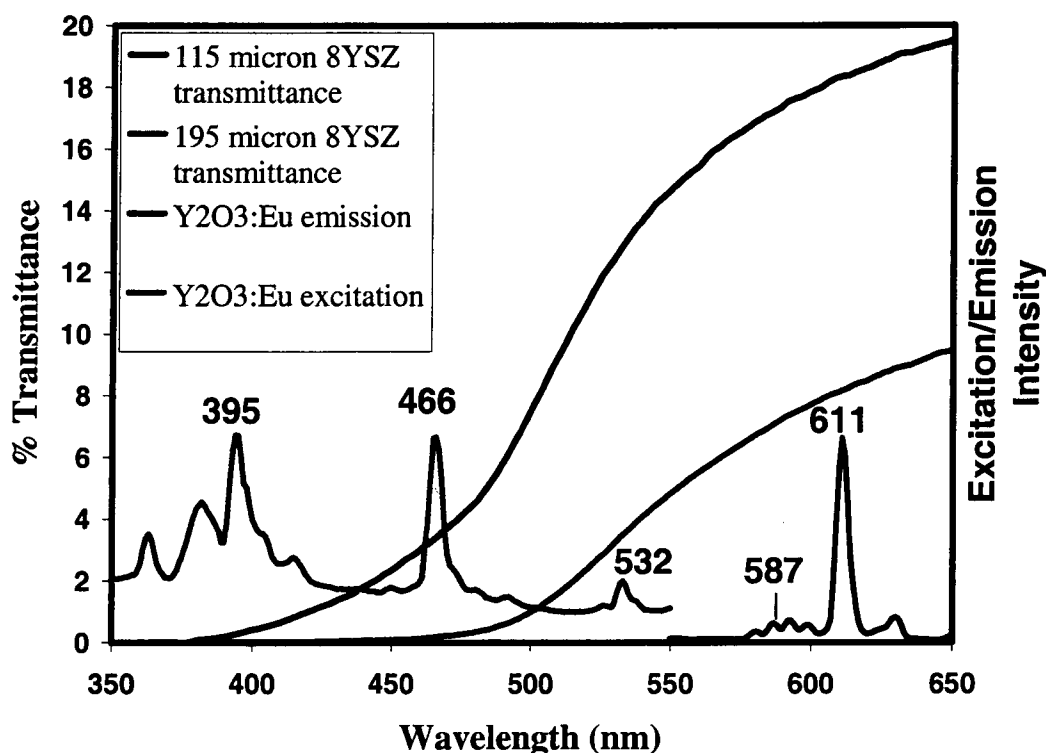


**Figure 1. Hemispherical transmittance plots for freestanding PS-8YSZ TBCs (115 and 195  $\mu\text{m}$  thick) along with excitation and emission spectra for  $\text{Y}_2\text{O}_3\text{:Eu}$ .**

doping of the YSZ TBC host without the introduction of a completely distinct phosphor layer that might be detrimental to TBC performance.

## EXPERIMENTAL PROCEDURE

### COATINGS

The PS-8YSZ TBC specimens were prepared by plasma-spraying 8YSZ powder (Zircoa, Inc.) onto sacrificial carbon disks (25.4 mm diameter x 3.2 mm thick). The estimated TBC thickness was 100  $\mu\text{m}$ . The  $\text{Y}_2\text{O}_3\text{:Eu}$  phosphor layer was painted onto the TBC surface using a 50:50 mixture (by volume) of HPC and LK (Zyp Coatings, Inc.) water-based binders. The paint containing approximately 20%  $\text{Y}_2\text{O}_3\text{:Eu}$  (6% Eu) powder by volume was applied to the TBC-coated carbon disks using a standard airbrush. The thickness of the applied phosphor paint was estimated to be approximately 25  $\mu\text{m}$ . Specimens were subsequently heated in air at 800°C to set the binder and to burn off the carbon substrate. The final freestanding specimens could then be oriented with the phosphor layer positioned either above or below the TBC.

### LUMINESCENCE SPECTROSCOPY AND DECAY TIME MEASUREMENTS

A Renishaw System 2000 Raman microscope was adapted to acquire both luminescence spectra and fluorescence decay time measurements. Figure 2 shows a simplified schematic of this Raman-

microscope-based system in which the following adaptations were made: (1) the original 514 nm continuous Ar ion laser was replaced by a low-power (4  $\mu\text{J}/\text{pulse}$ ) Nanogreen (model, NG-00321-110, JDS Uniphase) pulsed (5.2 kHz) 532 nm YAG:Nd laser to enable pulsed excitation, (2) a 532 nm longpass edge filter replaced the 514 nm notch filter, and (3) a photomultiplier tube (PMT; Hamamatsu Model HC125-01) was installed behind the angle-tunable filter wheel to detect the time-resolved fluorescence; the time-resolved fluorescence signal was collected by a 100 MHz digital oscilloscope (Agilent model 54622A) external to the spectrometer that was triggered by the laser pulse. The specimen was mounted in a hot stage (Linkam Model TS1500) attached to the stage of an optical microscope equipped with a 20x ultra-long working distance objective (Mitutoyo). The laser was defocused to a diameter of approximately 100  $\mu\text{m}$  to provide relative insensitivity to local inhomogeneities in the coating. With this configuration (Fig. 2), the phosphor layer emission spectra as a function of temperature were acquired with the translatable diverting mirror removed from the optical path so that the dispersion created by the grating is resolved by the position-sensitive (but not time-resolved) CCD detector. Without any realignment, refocusing, or sample repositioning, the fluorescence decay time measurements were acquired with the translatable mirror positioned to divert the optical path towards the filter wheel and PMT. The narrow bandpass (< 1 nm) angle-tunable filter could then be positioned to select any of the emission peaks observed in the phosphor emission spectra. To maximize signal-to-noise, the triggered decay-time measurements were averaged over 16384 laser pulses. In addition, a blank run with no excitation laser was run at each temperature to provide a baseline correction.

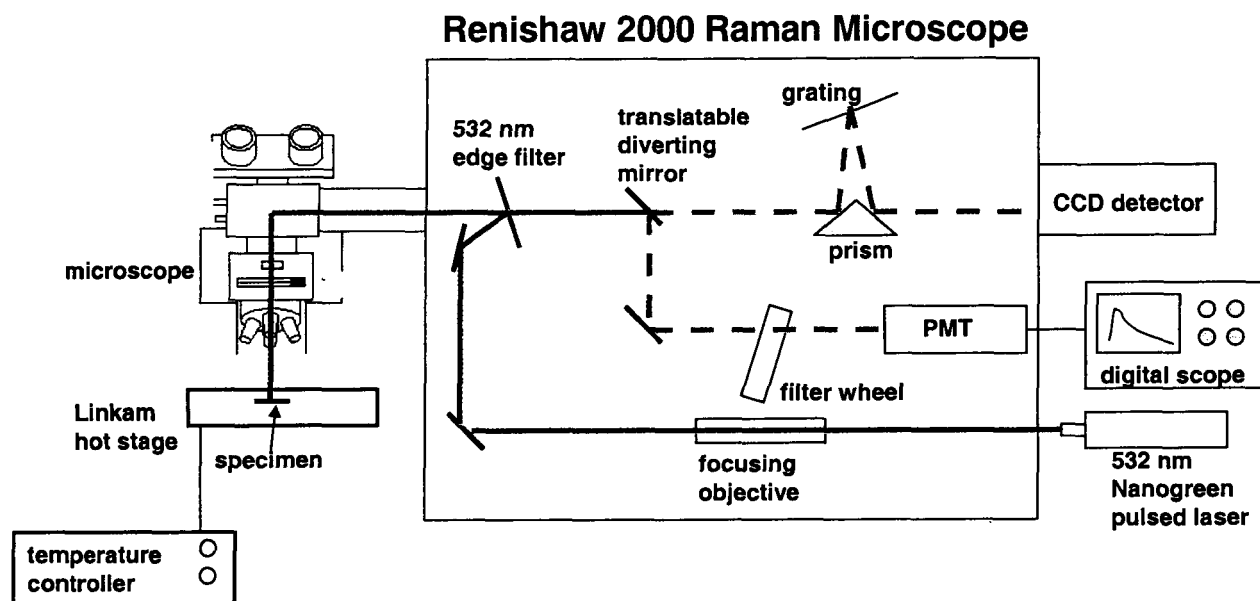


**Figure 2. Schematic of Raman-microscope-based system used to acquire both phosphor layer emission spectra and fluorescence decay time measurements as a function of coating temperature.**

## FLUORESCENCE DECAY TIME ANALYSIS

Inspection of the fluorescence decay curves for the primary 611 nm emission peak produced by the  $\text{Y}_2\text{O}_3\text{:Eu}$  phosphor (Figure 3) indicated that the decay curves could not be modeled by a simple exponential decay and that modeling should incorporate a rise time as well as a decay time. This observation is consistent with the report of a temperature and dopant-level dependent rise time for the 611 nm emission in  $\text{Y}_2\text{O}_3\text{:Eu}$  by Ranson et al. (ref. 8). The rise time was attributed to the relatively sluggish energy transfer between nearby  $\text{Eu}^{3+}$  ions sitting at inequivalent  $\text{Y}^{3+}$  symmetry sites (from  $^5\text{D}_1$  level of  $\text{Eu}^{3+}(\text{C}_{3i})$  to the  $^5\text{D}_0$  level of  $\text{Eu}^{3+}(\text{C}_2)$ ). The simple model proposed by Ranson et al. (ref. 8) to incorporate this slower energy transfer between inequivalent sites into the fluorescence decay behavior,  $I_{\text{emission}}(t)$ , was adopted here:

$$I_{\text{emission}}(t) = [c_1 + c_2[1 - e^{\frac{-t}{\tau_{\text{rise}}}}]]e^{\frac{-t}{\tau_{\text{decay}}}} \quad (1)$$

where  $I_{\text{emission}}(t)$  is the emission intensity as a function of time,  $c_1$  and  $c_2$  are scaling constants, and  $\tau_{\text{rise}}$  and  $\tau_{\text{decay}}$  are the rise time and decay time, respectively. The rise time, decay time, and two scaling constants were determined by fitting Equation 1 to the decay-time measurements using the Solver utility in Microsoft Excel. Figure 3 shows a curve that was fit to the data in this manner.

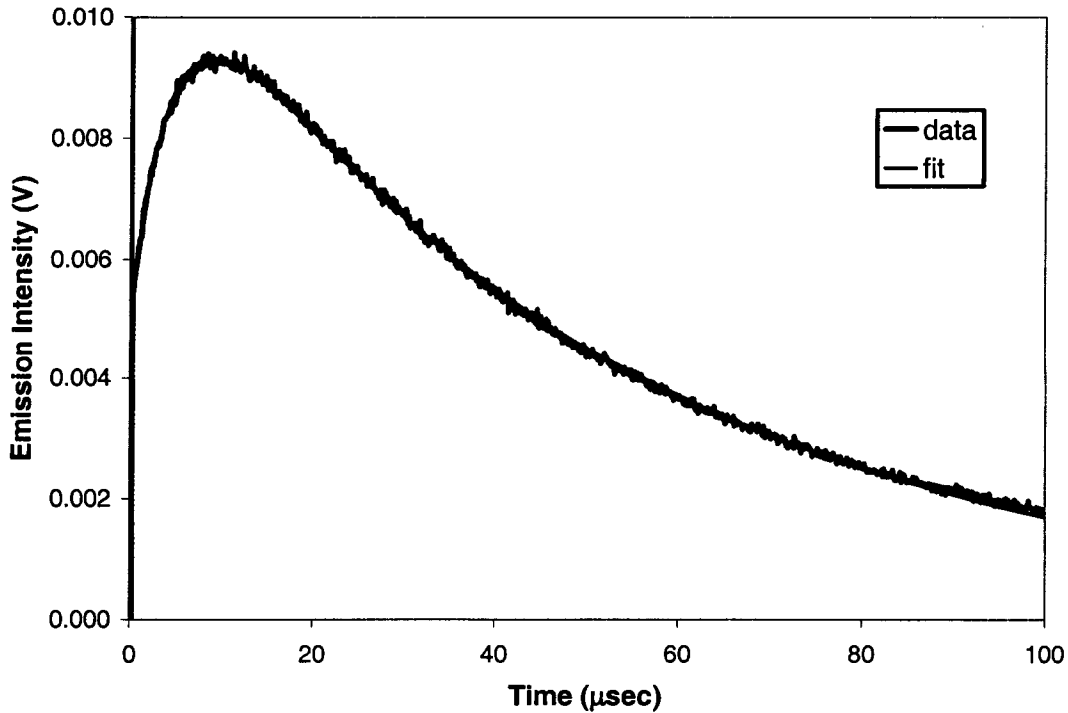


**Figure 3. Fluorescence decay curve at 700°C from  $\text{Y}_2\text{O}_3\text{:Eu}$  layer beneath freestanding 100- $\mu\text{m}$  thick PS-8YSZ (blue). The red curve is the result of fitting Equation 1 to the data.**

## RESULTS

The temperature dependence of the emission spectra from the  $\text{Y}_2\text{O}_3\text{:Eu}$  layer (on top of the TBC) is shown in Figure 4. For comparison, the spectra were normalized to display similar maximum intensities; actual signals decreased significantly at higher temperatures. The 611 nm emission peak shows a small but consistent displacement to longer wavelengths as well as a significant broadening with increasing temperature. The 611 nm emission peak has by far the greatest intensity at low temperatures; however, it is interesting to note that the 587 nm emission peak is comparable or greater at 1000°C. While the 611 nm emission peak was used for the fluorescence decay time measurements, these results indicate that the 587 nm emission peak should be considered for measurements above 1000°C where it may suffer less competition from the thermal radiation background (as seen in the slope of the 1000°C plot in Fig. 4). The 587 nm peak also shows broadening with increasing temperature, but shows a consistent displacement to shorter wavelengths with increasing temperature.

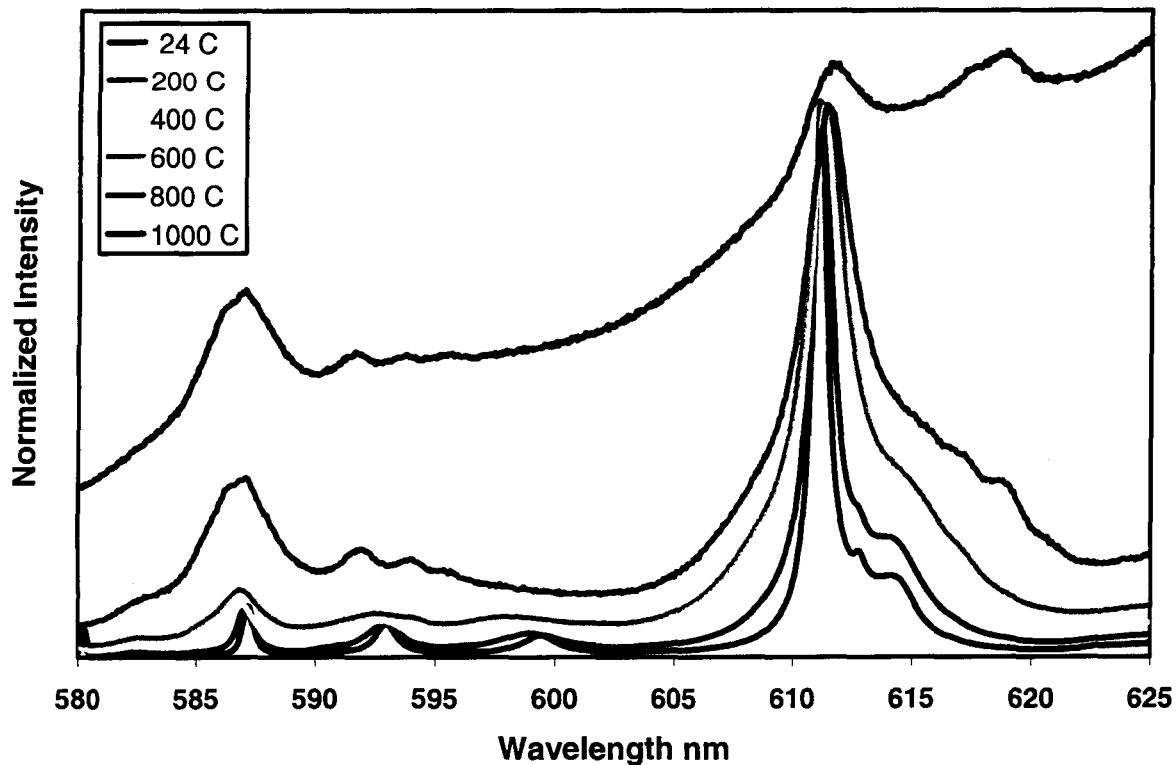


**Figure 4. Emission spectra as a function of temperature for  $\text{Y}_2\text{O}_3\text{:Eu}$  layer above freestanding 100- $\mu\text{m}$  thick PS-8YSZ TBC.**

Figure 5 shows that the intensity of the observed 611 nm emission (room temperature) from the  $\text{Y}_2\text{O}_3\text{:Eu}$  layer is reduced considerably (factor of  $\sim 30$ ) when the phosphor layer is below the 100- $\mu\text{m}$  thick TBC compared to when the phosphor layer is above the TBC. This reduction is due to the attenuation of both

the 532 nm excitation and the 611 nm emission intensities (see Fig. 1). However, even with this significant reduction, the 611 nm emission from the phosphor below the TBC was still easily detected and the reduced intensity was sufficient to perform fluorescence decay time measurements.

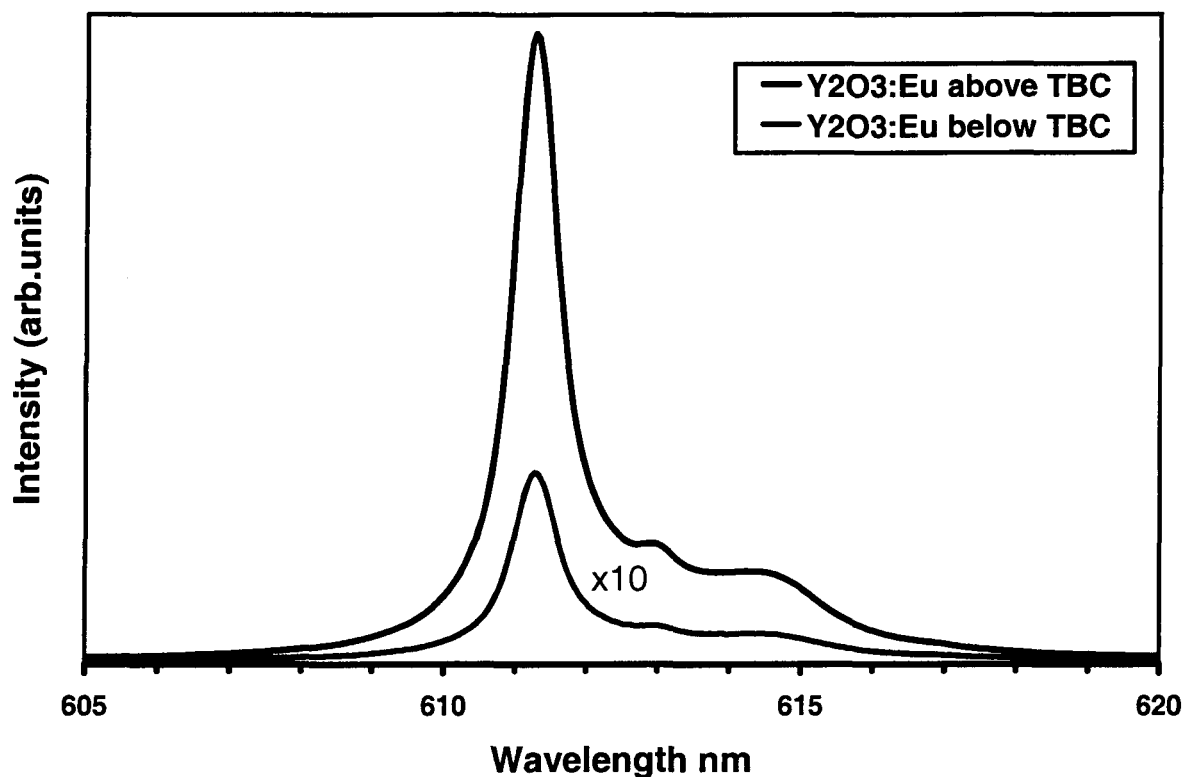


**Figure 5.** Comparison of 611 nm emission intensity at room temperature for  $\text{Y}_2\text{O}_3\text{:Eu}$  layer above versus below freestanding 100- $\mu\text{m}$  thick PS-8YSZ TBC. Emission spectrum for  $\text{Y}_2\text{O}_3\text{:Eu}$  below the TBC was multiplied x10 for easier comparison.

Fluorescence decay time measurements were performed for both orientations of the freestanding coatings: with the  $\text{Y}_2\text{O}_3\text{:Eu}$  phosphor layer above the TBC and with the phosphor layer below the TBC. For each orientation, decay time measurements were performed as a function of coating temperature. Measurements were obtained at 50°C intervals up to 600°C and then at 20°C intervals up to 1000°C. The hot stage was held at each selected temperature for a minimum of 10 min before decay time measurements were acquired. Both  $\tau_{\text{decay}}$  and  $\tau_{\text{rise}}$  were determined by fitting Equation 1 to the fluorescence decay data and are displayed in Figure 6. Figure 6 shows that there was good match between the values determined for the  $\text{Y}_2\text{O}_3\text{:Eu}$  layer above the TBC and the values determined for the  $\text{Y}_2\text{O}_3\text{:Eu}$  layer beneath the TBC, indicating that the temperature calibrations of the fluorescence decay time are equivalent and that despite the signal attenuation due to the overlying TBC, the phosphor layer located below the TBC still functions as an effective temperature probe.

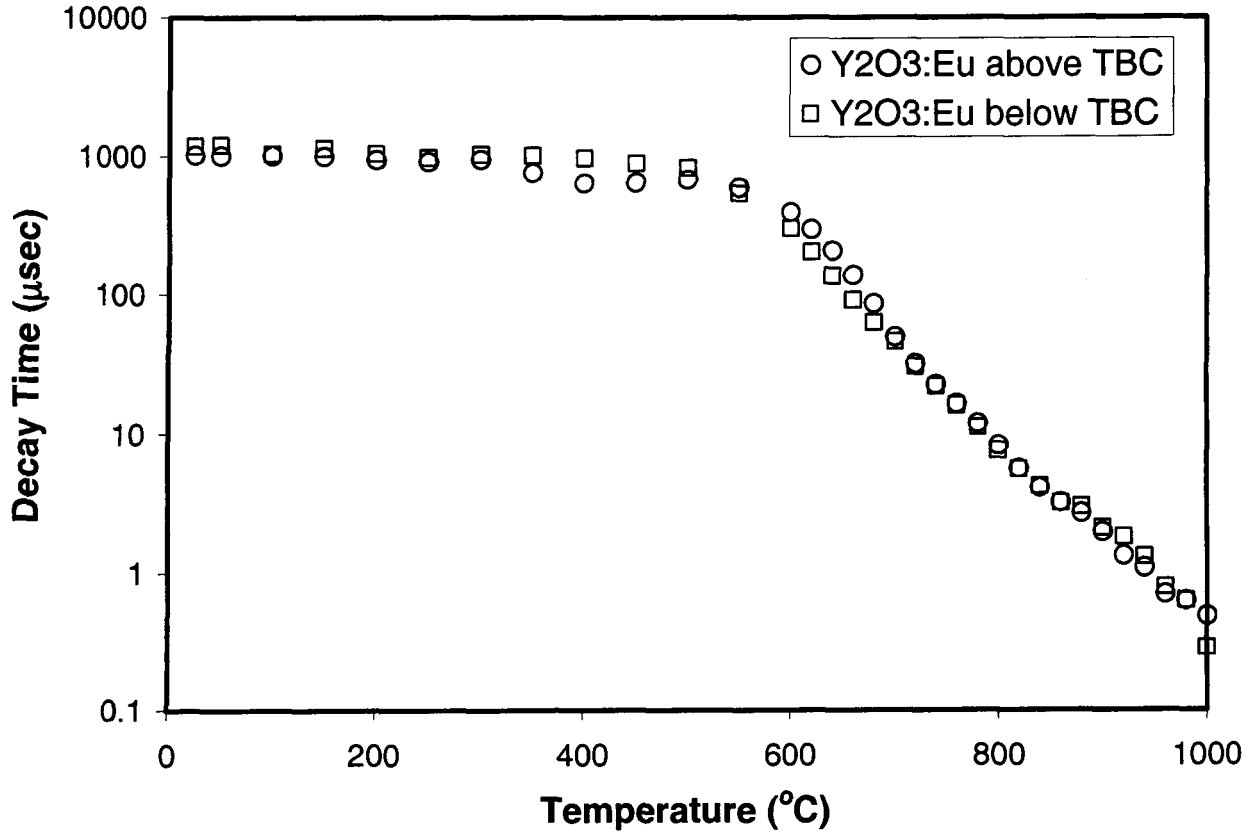


**Figure 6. Decay time ( $\tau_{\text{decay}}$ ) as a function of coating temperature for  $\text{Y}_2\text{O}_3\text{:Eu}$  layer above versus below freestanding 100- $\mu\text{m}$  thick PS-8YSZ TBC.**

Figure 6 shows that  $\tau_{\text{decay}}$  is relatively insensitive to temperature at temperatures below 500°C and therefore does not provide an effective temperature probe at these lower temperatures. However, Figure 7 shows that  $\tau_{\text{rise}}$  has a significantly higher sensitivity to temperature below 500°C and offers the potential of providing temperature indication in this range. Above 500°C, the much greater temperature sensitivity of  $\tau_{\text{decay}}$  “kicks in” and makes  $\tau_{\text{decay}}$  a much better temperature indicator than  $\tau_{\text{rise}}$ . Also, above 800°C, within the limitations of the instrumentation used here,  $\tau_{\text{rise}}$  becomes too short to determine accurately.



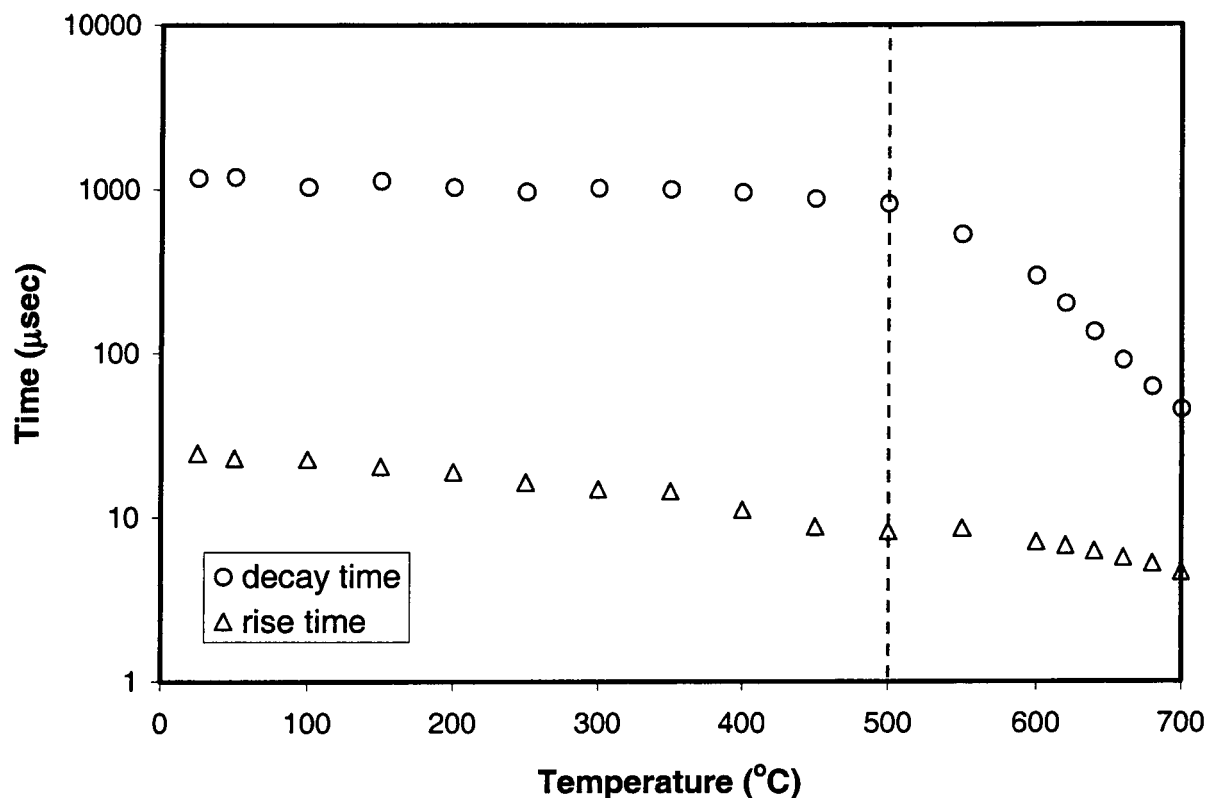


**Figure 7. Comparison of decay time ( $\tau_{\text{decay}}$ ) versus rise time ( $\tau_{\text{rise}}$ ) as a function of temperature determined from decay of 611 nm emission from  $\text{Y}_2\text{O}_3\text{:Eu}$  layer.**

## DISCUSSION OF POTENTIAL IMPROVEMENTS

While Figure 6 demonstrates the successful application of a  $\text{Y}_2\text{O}_3\text{:Eu}$  phosphor layer for through-the-thickness TBC temperature measurements up to 1000°C, TBCs are subjected to temperatures up to 1200°C in current turbine engine designs, and future generations of TBCs will be required to sustain even higher temperatures. To achieve these higher temperature measurements, further optimization of the fluorescence decay measurements will be required. Measurements above 1000°C proved difficult because the fluorescence intensity decreases dramatically with increasing temperature resulting in poor signal-to-noise ratio and the decay time becomes very short ( $< 1 \mu\text{sec}$ ). The loss in fluorescence signal intensity could be offset through use of a pulsed laser with higher power pulses than the very low power ( $4 \mu\text{J/pulse}$ ) laser used for this report; several orders of magnitude increase in signal could easily be achieved through a higher power laser. Another approach to increase the signal-to-noise ratio would be to take better advantage of the available signal by tailoring the bandpass filter to match the width of the emission peak. In the current design (Fig. 2), the narrow bandpass ( $< 1 \text{ nm}$ ) angle-tunable filter only transmits a small fraction of the emission band, especially at high temperatures where the emission peak becomes quite broad (Fig. 4).

Another difficulty in extending thermographic-phosphor-based temperature measurements to higher temperatures is the competition from the thermal radiation background. In this aspect, it was found that the microscope-based light collection configuration employed for this report excelled in minimizing the thermal radiation background in the fluorescence decay measurements. Even at 1000°C, the thermal radiation background was a negligible contribution to the fluorescence decay measurements (in contrast to the emission spectra where the thermal radiation background was quite noticeable (Fig. 4)). This suppression of thermal radiation background is proposed to be due to the microscope-based configuration that restricts collection of thermal radiation to a small area around the excitation laser spot.

Finally, thermographic-phosphor-based temperature measurements may interfere with the TBC performance (bonding, lifetime, and thermal protection) when a distinct  $\text{Y}_2\text{O}_3\text{:Eu}$  phosphor layer is inserted into the TBC/substrate system. For retaining TBC performance, a much more acceptable solution would be to introduce layered low-level doping of Eu into the 8YSZ material of which the TBC is composed. As previously noted, this approach should succeed since YSZ:Eu has been demonstrated to be an effective thermographic phosphor (ref. 6).

## SUMMARY

The use of thermographic phosphor ( $\text{Y}_2\text{O}_3\text{:Eu}$ ) fluorescence decay time measurements were demonstrated for the first time for through-the-thickness temperature readings up to 1000°C with the phosphor layer residing beneath a 100- $\mu\text{m}$  thick freestanding PS-8YSZ TBC. These depth-penetrating temperature measurements were accomplished by selecting a phosphor,  $\text{Y}_2\text{O}_3\text{:Eu}$ , that has a minor excitation peak at 532 nm and emission peaks at 587 and 611 nm that could all be transmitted through the TBC. In particular, switching from the commonly used excitation peak at 267 nm (where the TBC is opaque) to the excitation peak at 532 nm allows sufficient transmittance of the excitation wavelength. The adaptation of a Raman microscope was found to be especially convenient for sequentially obtaining phosphor layer emission spectra as a function of temperature and then to use these spectra to select emission peaks for performing fluorescence decay-time measurements with the same instrument. Results of these measurements indicated:

- Successful temperature measurements up to 1000°C with the phosphor layer underneath a 100- $\mu\text{m}$  thick TBC despite attenuation of the detected fluorescence intensity by a factor of  $\sim 30$  due to the overlying TBC.
- Equivalent temperature calibrations of fluorescence decay times for the phosphor layer above and below the TBC.
- Rise time,  $\tau_{\text{rise}}$ , was a better temperature indicator below 500°C; decay time,  $\tau_{\text{decay}}$ , was a better indicator above 500°C.
- The emission peak at 587 nm should be considered for potential advantages over the emission peak at 611 nm for temperature measurements above 1000°C.
- In addition to using the temperature dependence of  $\tau_{\text{decay}}$ , both the 587 and 611 nm emission peaks show a temperature dependence of peak position and width that could be used for temperature measurements.

In conclusion, the successful demonstration of the use of thermographic phosphors to achieve depth-penetrating temperature measurements shows significant potential for the incorporation of luminescent

species into TBCs to add sensing functions that will provide information about temperature gradients and coating integrity.

## REFERENCES

1. D. Zhu and R.A. Miller, Thermal-Barrier Coatings for Advanced Gas-Turbine Engines," MRS Bull., 25(7), 43-47 (2000).
2. K.W. Tobin, S.W. Allison, M.R. Cates, G.J. Capps, D.L. Beshears, M. Cyr, and B.W. Noel, "High-Temperature Phosphor Thermometry of Rotating Turbine Blades," AIAA J., 28(8), 1485-1490 (1990).
3. J.R. Markham and K. Kinsella, "Thermal Radiative Properties and Temperature Measurement from Turbine Coatings," Int. J. Thermophysics, 19(2), 537-545 (1998).
4. H. Latvakoski, J. Markham, M. Borden, T. Hawkins, and M. Cybulsky, "Measurement of Advanced Ceramic Coated Superalloys with a Long Wavelength Pyrometer, AIAA Report 2000-2212, American Institute of Aeronautics, 21<sup>st</sup> AIAA Aerodynamic Measurement Technology and Ground Testing Conference, June 2000, Denver, CO.
5. S.W. Allison, D.L. Beshears, M.R. Cates, B.W. Noel, and W.D. Turley, "Taking an Engine's Temperature," Mech. Eng., 119(1), 72-74 (1997).
6. J.P. Feist and A.L. Heyes, "Development of the Phosphor Thermometry Technique for Applications in Gas Turbines," 10<sup>th</sup> International Symposium on Applications of Laser Techniques to Fluid Mechanics, Lisbon, Portugal, 2000.
7. S. D. Alaruri, A.J. Brewington, M.A. Thomas, and J.A. Miller, "High-Temperature Remote Thermometry Using Laser-Induced Fluorescence Decay Lifetime Measurements of Y<sub>2</sub>O<sub>3</sub>:Eu and YAG:Tb Thermographic Phosphors," IEEE Trans. Instrum. Measurement, 42(3), 735, 739 (1993).
8. R.M. Ranson, E. Evangelou, and C.B. Thomas, "Modeling the Fluorescent Lifetime of Y<sub>2</sub>O<sub>3</sub>:Eu," Appl. Phys. Lett., 72(21), 2663-2664 (1998).